Something about Polarisation Spectroscopy

Joshua Torrance

October 15, 2014

Abstract

By capitalising on the demonstrably high bandwidth of polarisation spectroscopy locking systems it it possible to achieve linewidths of 15 kHz using standard diode lasers.

1 Introduction

Frequency stabilisation is essential to numerous applications such as the cooling and trapping of atoms, optical fibre communications and metrology [1,2]. Polarisation spectroscopy has much in common with the standard laser locking techinique, saturated absorption spectroscopy [3–5]. Both techniqies provide a good frequency reference that can be used to lock lasers to atomic resonaces.

Narrow linewidth is good...

Narrow linewidths are important for applications in metrology [6], atomic clocks [7], atomic trapping and cooling [8–10] and high resolution spectroscopy [11].

Current linewidths are...

Current techniques range from simple laser stabilisation with saturated absorption which can achieve linewidths in the region of 150kHz [12] to elaborate experiments involved extremely high finesse cavities that are able to achieve sub-Hertz linewidths with diode lasers using Pound-Drevor-Hall (PDH) locking. [13]

History...

Polarisation spectroscopy was first presented as an alternative to saturated absorption spectroscopy with higher signal to noise ratios [14]. Later developments on the technique use a balanced polarimeter instead of crossed polarisers in order to obtain a background-free dispersion signal which is suitable for high-speed and more robust stabilisation [15].

Phase stabilisation dipole response time

Polarisation spectroscopy can be used for phase stabilisation due to the finite response time of the atomic dipoles to pertubation in the laser phase [16]. I don't like this sentence. Also what about response time of sub-level population? Similar to [17] although that one is static not dynamic. What's the response time for sub-level population response?

Description of pol spec with reference to papers that explain it in detail.

Experimental setup

A schematic diagram of the experimental setup can be seen in figure 2. An external cavity diode laser (ECDL) (Toptica DL Pro) operating at 780nm with a diode of some description which outputs X mW. This light is then split by a polarising beam splitter (PBS) and the light transmitted through the PBS passes through a acousto-optical modulator (AOM) twice before entering a fibre to the cavity linewidth setup as shown in figure 1. The light reflected through the PBS goes through an optical fibre to the polarisation specroscopy setup shown in figure 2.

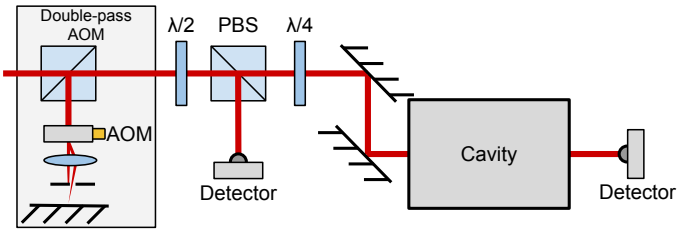

Figure 1: A simplified schemeatic diagram of the cavity setup used to measure linewidth.

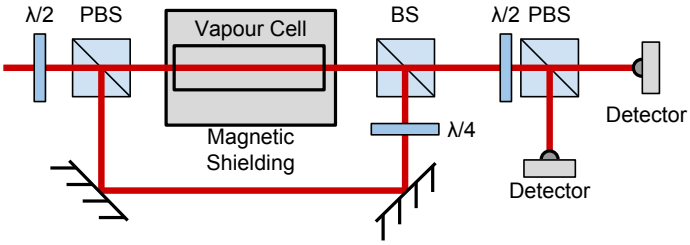

Figure 2: A simplified schematic diagram of the polarisation spectroscopy setup.

Bandwidth (and data)
Phase lead? (and details and data)
Linewidth measurement (and data)
Conclusion

2 Papers

- Oringal Wieman and Hänsch paper [14].
- Analogy to PDH explaining phase memory and fast response in [16].
- Mathematics on polarisation rotation through the sample and simulation of pumping transitions in [17].
- Bloch equations to population anisotropy [18]
- 'Bi-polarisation spectroscopy' two pairs of beams through sample [19].

- Rate equations used to calculate spectra and good comparison to experiment [20].

3 Polarisation Spectroscopy Theory

Simplistic view:

- Circular pump beam travels through the sample.
- When the frequency is tuned to a transition the atoms are pumped to a magnetic substate.
- The linearly polarised probe beam can be decomposed into σ^+ and σ^-. Each of these components experience a differenct absorption coefficient and different refractive indices from the nonisotropic saturation of the magnetic sublevels caused by the pump. This results in the probe beam becoming eliptically polarised and rotating the major axis.
- This rotation is easily observed by the analyser.

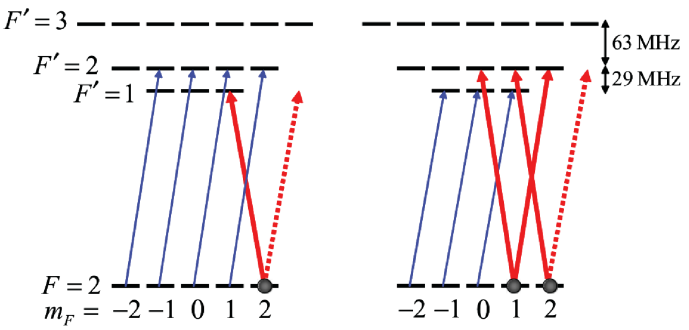

Figure 3: Two pump probe configurations contributing to the crossover transition. The blue thin arrows indicate the transitions by the σ^+ pump (spin-polarising) beam which optically pumps the atom to the $m_F = 1$ or $m_F = 2$ states. The red thick arrows indicate the transitions by the probe beam. The σ^+ transitions which are not allowed for the pin-polarised atom are indicated by the red dotted arrows. In both configurations, the σ^- component of the probe beam predominantly interacts with the atoms, resulting in circular birefringence for the probe beam.

3.1 Birefringence in the Atomic Sample

The initial state of the probe beam with linear polarisation in a plane at an angle ϕ from the x axis can be expressed as

$$\boldsymbol{E} = \begin{bmatrix} E_x \\ E_y \end{bmatrix} = E_0 \begin{bmatrix} \cos\phi \\ \sin\phi \end{bmatrix}. \tag{1}$$

This can be reexpressed in terms of the circular polarisation basis vectors

$$\boldsymbol{E} = E_0 \begin{bmatrix} \cos\phi \\ \sin\phi \end{bmatrix} = E_0 \left\{ \frac{e^{-i\phi}}{2} \begin{bmatrix} 1 \\ i \end{bmatrix} + \frac{e^{i\phi}}{2} \begin{bmatrix} 1 \\ -i \end{bmatrix} \right\} \tag{2}$$

After the beam has passed through the cell windows and atomic sample the electric field of the probe is

$$\begin{aligned} \boldsymbol{E} = E_0 \Bigg\{ & \frac{e^{-i\phi}}{2} \begin{bmatrix} 1 \\ i \end{bmatrix} e^{-ik_+ L} e^{-\alpha_+ L/2} e^{-ik_{w+} l} + \\ & \frac{e^{i\phi}}{2} \begin{bmatrix} 1 \\ -i \end{bmatrix} e^{-ik_- L} e^{-\alpha_- L/2} e^{-ik_{w-} l} \Bigg\} \end{aligned} \tag{3}$$

where $k_\pm = \frac{\omega}{c} n_\pm$, $n_\pm$ are the refractive indices of the gas for the circular polarisation components which drive $\sigma_\pm$ transitions; $\alpha_\pm$ are the corresponding absorption cooefficients and the $k_\pm = \frac{w}{c} n_{w\pm}$ terms describe te phase change picked up while traversing the window (windows??) of width l. The refractive indices are complex and can be written as $n_{w\pm} l = b_{R\pm} - i\frac{c}{\omega} b_{l\pm}$. We can rewrite the expression as

$$\begin{aligned} \boldsymbol{E} = E_0 \exp & \left\{ -i \left[\frac{\omega}{c}(nL + b_R) - i b_l - i\frac{\alpha L}{2} \right] \right\} \\ & \left\{ \frac{e^{-i\phi}}{2} \begin{bmatrix} 1 \\ i \end{bmatrix} e^{+i\Omega} + \frac{e^{i\phi}}{2} \begin{bmatrix} 1 \\ -i \end{bmatrix} e^{-i\Omega} \right\}. \end{aligned} \tag{4}$$

where,

$$\begin{aligned} \Omega &= \frac{\omega}{2c}(\Delta n L + \Delta b_R) - i\left(\frac{L}{4}\delta\alpha_{\frac{1}{2}}\delta b_l\right), \\ n &= \frac{1}{2}(n_+ + n_-), \\ \alpha &= \frac{1}{2}(\alpha_+ + \alpha_-), \\ b_R &= \frac{1}{2}(b_{R+} + b_{R-}), \\ b_l &= \frac{1}{2}(b_{l+} + b_{l-}) \\ \Delta n &= n_+ - n_-, \\ \Delta\alpha &= \alpha_+ - \alpha_-, \\ \Delta b_R &= b_{R+} - n_{R-}, \\ \Delta b_l &= b_{l+} - b_{l-}. \end{aligned} \tag{5}$$

The polarising beam splitter cube in the analyser will split the probe beam into its horizontal (x) and vertical (y) components and the difference in intensity gives the polarisation spectroscopy signal:

$$\begin{aligned} I_{signal} &= I_y - I_x \\ I_{signal} &= I_0 e^{-\alpha L - 2b_l} \cos\left(2\phi + L\Delta n\frac{\omega}{c} + \Delta b_R \frac{\omega}{c}\right) \end{aligned} \tag{6}$$

Here, I_0 is the intensity of the probe beam before the cell.

4 Phase Through an Atomic Sample

Apparently [21], the phase accumulated by a laser passing though an atomic sample is

$$\phi(\vec{x}) = \frac{2\pi}{\lambda} \int_{-\infty}^{\infty} [n(\vec{r}) - 1]\, dz \tag{7}$$

where the refractive index for a two-level atom is [22]

$$n(\vec{r}) = 1 + N(\vec{r})\frac{\sigma_0\lambda}{4\pi}\frac{i-2\Delta}{1+4\Delta^2} \tag{8}$$

σ_0 is the atomic cross-section. $\Delta = (\omega - \omega_0)/\Gamma_{excited}$ is the detuning.

I'm not currently sure where equation 7 comes from but the two-level refractive index comes from. It's probably derivable from common sense. Equation 8 comes from Bloch equations.

Combining 7 and 8,

$$\begin{aligned}\phi(\vec{r}) &= \frac{2\pi}{\lambda}\int\left[1 + N(\vec{r})\frac{\sigma_0\lambda}{4\pi}\frac{i-2\Delta}{1+4\Delta^2} - 1\right]dz \\ &= \frac{2\pi}{\lambda}\int\left[N(\vec{r})\frac{\sigma_0\lambda}{4\pi}\frac{i-2\Delta}{1+4\Delta^2}\right]dz\end{aligned} \tag{9}$$

If a homogenous beam (Δ is constant, any intensity reliance?) and sample distribution ($N(\vec{r})$ is constant) are assumed then

$$\begin{aligned}\phi(\vec{r}) &= \frac{2\pi}{\lambda}\frac{\sigma_0\lambda}{4\pi}\frac{i-2\Delta}{1+4\Delta^2}N\int 1\,dz \\ &= \frac{\sigma_0}{2}\frac{i-2\Delta}{1+4\Delta^2}NL\end{aligned} \tag{10}$$

where L is the length of the atomic sample.

$$\sigma_0 = \frac{2J'+1}{2J+1}\frac{\lambda^2}{2\pi} \tag{11}$$

5 Pound-Drevor-Hall

Probably best to follow Torii and compare to PDH in order to explain high bandwidth:

If a laser of frequency ω_L is incident on a cavity with a resonance frequency of ω_C with full-width half maximum (FWHM) resonance width $\Delta\omega_C$. Just outside the cavity the complex amplitude of the incident field can be expressed as $E_I = E_0 exp(i\omega_L t)$. E_R, the reflected field, is the sum of the leakage field from the cavity E_L and the promptly reflected field off the input mirror E_P. For high finesse cavities $E_P \approx E_I$ if for simplicity we assume that there is no phase chance upon reflection. The complex stead-state aplitude of the reflected field is then:

$$E_R = E_P + E_L = \left(1 - \frac{1-R_1}{1-R}\frac{1-ix}{1+x^2}\right)E_I \tag{12}$$

where R_1 is the intensity reflectivity of the input mirror, R is the amplitude ration between successive round-trips in the cavity, and $x = (\omega_L - \omega_C)/(\Delta\omega_C/2)$ is a normalised laser frequency detuning from the cavity resonance.

6 Bandwidth

What is bandwidth?

In signal processing bandwidth is the difference between the upper and lower frequencies in a spectrum. In the context of error signals for laser locking the bandwidth is the difference between the lowest frequency (usually 0Hz) and the highest frequency at which the error is above the noise.

Why do we get high bandwidth?

With PDH the high-bandwidth comes from the cavity response time, $\tau_C = 1/\Delta\omega_C$. The field inside the cavity cannot follow the phase jump of the laser and the leakage field shiftsin the rotating complex plane.

Similarly with Polarisation Spectroscopy the high-bandwidth comes from the atomic coherence time $\tau_A = 1/\Gamma$. The atomic dipole oscillations are unable to follow sudden phase shifts in the incident field.

7 Phase Lead

By the time the error signal reaches the diode the high frequency components of the error signal are no longer appropriate given the time delay in the electrics and the response time of the diode.

8 Measurements

8.1 Bandwidth

Bandwidth can be measured by comparing the spectrum of the error signal on the resonance of interest to a background signal off the resonance as shown in 4.

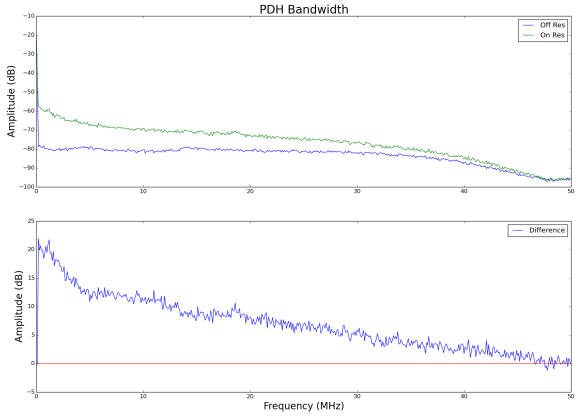

Figure 4: Something something bandwidth.

8.2 Linewidth Measurements

Words are hard. The next explanation feels clumsy to me.

By directing a locked laser's light through a high finesse cavity and either scanning the laser's frequency with an AOM or scanning the cavity's length with a piezo attached

to one of the mirrors it is possible to get a trace of the convolution of the cavity's Airy transmission function T and the laser's lineshape L.

$$T(\delta) = \frac{1}{1 + Fsin^2(\delta)} \tag{13}$$

$$L(\delta) = \frac{\sigma^2}{\delta^2 + \sigma^2} \tag{14}$$

Where F is the coefficient of finesse for the cavitiy, δ is the frequency detuning of the laser from the cavity's resonance and 2σ is the FWHM of the Lorentzian.

Convolving a cavity with a finesse of 20942 (which has a transmision function with a FWHM of 71.6kHz) with a Lorentzian with a FWHM of 10kHz produces an approximately Lorentzian line with a FWHM of 81.6KHz as shown in figure 5.

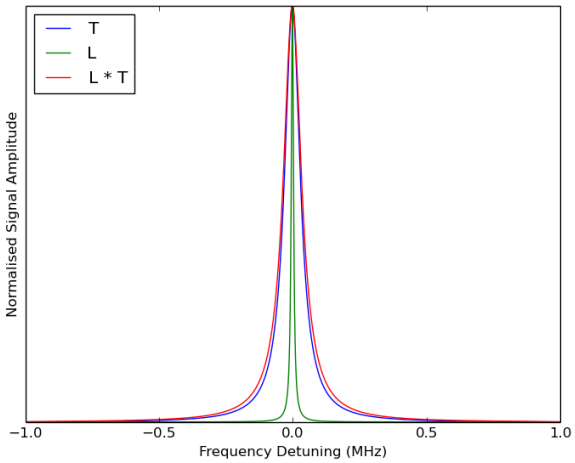

Figure 5: The blue line shows the transmision function for a acvity with a finesse of 20942. The green line shows a Lorentzian with a FWHM of 10kHz. The red line shows the convolution of the blue and green lines and represents the signal that would be measured as transmitting through a cavity illuminated by a laser with a lineshape given by the green line.

If, instead of scanning the laser the frequency is set so that the frequency is at a point where the the transmission through the cavity is partway up the side of the peak then the subsequent fluctuations in amplitude can be mapped to a Lorentzian fitted to the peak and thus transformed to a frequency. The distribution of frequencies in turn provide can be used to calculate the linewidth of the laser.

Using this technique linewidths of 11.72 kHz have been measured using the experimental setup described somewhere else in this document.

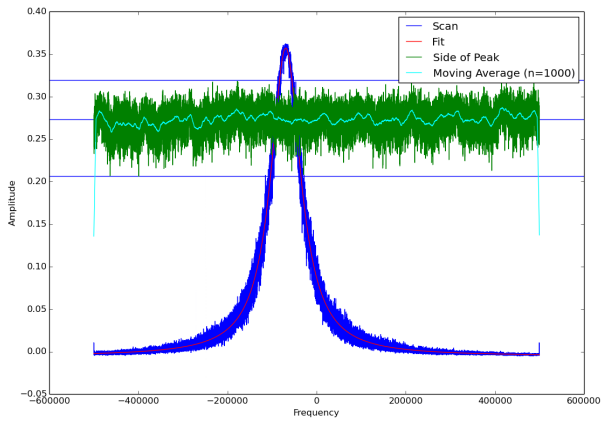

Figure 6: A polarisation spectroscopy locked laser scanned through a high finesse cavity (blue line). The green line is the same laser, no longer scanning, with it's frequency adjusted such that it is on the side of the transmission peak.

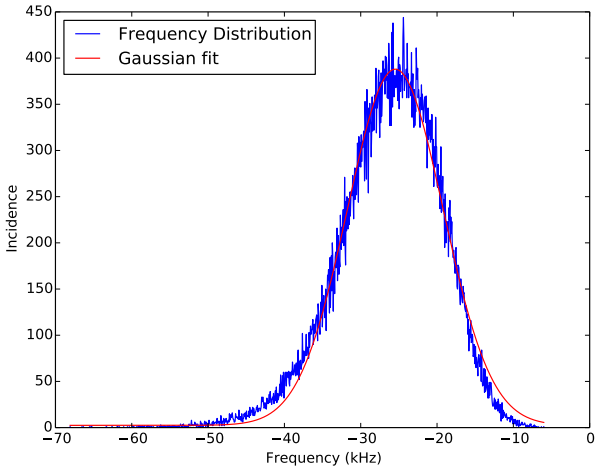

Figure 7: The blue line shows the frequency distribution of the feen line in figure 6. The red line is a Gaussian fit which has a FWHM of 11.72 kHz.

References

[1] H. J. Metcalf and P. van der Straten. *Laser Cooling and Trapping*. Springer, 1999.

[2] Wolfgang Demtröder. *Laser Spectroscopy 1*. 5 edition, 2014.

[3] L. P. Maguire, R. M. W. van Bijnen, E. Mese, and R. E. Scholten. Theoretical calculation of saturated absorption spectra for multi-level atoms. *Journal of Physics B: Atomic, Molecular and Optical Physics*, 39(12):2709–2720, June 2006.

[4] S. Haroche and F. Hartmann. Theory of saturated-absorption line shapes. *Physical Review A*, 6(4):1280–1300, October 1972.

[5] D. W. Preston. Doppler-free saturated absorption: Laser spectroscopy. *American Journal of Physics*, 64(11):1432, 1996.

[6] Jun Ye, H. J. Kimble, and Hidetoshi Katori. Quantum state engineering and precision metrology using state-insensitive light traps. *Science*, 320(5884):1734–1738, June 2008.

[7] A. D. Ludlow, T. Zelevinsky, G. K. Campbell, S. Blatt, M. M. Boyd, M. H. G. de Miranda, M. J. Martin, J. W. Thomsen, S. M. Foreman, Jun Ye, T. M. Fortier, J. E. Stalnaker, S. A. Diddams, Y. Le Coq, Z. W. Barber, N. Poli, N. D. Lemke, K. M. Beck, and C. W. Oates. Sr lattice clock at 1 × 10–16 fractional uncertainty by remote optical evaluation with a ca clock. *Science*, 319(5871):1805–1808, March 2008.

[8] S. Uetake, A. Yamaguchi, S. Kato, and Y. Takahashi. High power narrow linewidth laser at 556 nm for magneto-optical trapping of ytterbium. *Applied Physics B*, 92(1):33–35, July 2008.

[9] Li Ye, Lin Yi-Ge, Zhao Yang, Wang Qiang, Wang Shao-Kai, Yang Tao, Cao Jian-Ping, Li Tian-Chu, Fang Zhan-Jun, and Zang Er-Jun. Stable narrow linewidth 689 nm diode laser for the second stage cooling and trapping of strontium atoms. *Chinese Physics Letters*, 27(7):074208, July 2010.

[10] Daisuke Akamatsu, Yoshiaki Nakajima, Hajime Inaba, Kazumoto Hosaka, Masami Yasuda, Atsushi Onae, and Feng-Lei Hong. Narrow linewidth laser system realized by linewidth transfer using a fiber-based frequency comb for the magneto-optical trapping of strontium. *Optics Express*, 20(14):16010, July 2012.

[11] R. J. Rafac, B. C. Young, J. A. Beall, W. M. Itano, D. J. Wineland, and J. C. Bergquist. Sub-dekahertz ultraviolet spectroscopy of 199hg+. *Physical Review Letters*, 85(12):2462–2465, September 2000.

[12] C. J. Cuneo, Jeffery J. Maki, and D. H. McIntyre. Optically stabilized diode laser using high-contrast saturated absorption. *Applied Physics Letters*, 64(20):2625–2627, May 1994.

[13] A. D. Ludlow, X. Huang, M. Notcutt, T. Zanon-Willette, S. M. Foreman, M. M. Boyd, S. Blatt, and J. Ye. Compact, thermal-noise-limited optical cavity for diode laser stabilization at 1×10^{-15}. *Optics Letters*, 32(6):641, 2007.

[14] C. Wieman and T. W. Hänsch. Doppler-free laser polarization spectroscopy. *Physical Review Letters*, 36(20):1170–1173, May 1976.

[15] Yutaka Yoshikawa, Takeshi Umeki, Takuro Mukae, Yoshio Torii, and Takahiro Kuga. Frequency stabilization of a laser diode with use of light-induced birefringence in an atomic vapor. *Applied Optics*, 42(33):6645, 2003.

[16] Yoshio Torii, Hideyasu Tashiro, Nozomi Ohtsubo, and Takatoshi Aoki. Laser-phase and frequency stabilization using atomic coherence. *Physical Review A*, 86(3):033805, September 2012.

[17] C. P. Pearman, C. S. Adams, S. G. Cox, P. F. Griffin, D. A. Smith, and I. G. Hughes. Polarization spectroscopy of a closed atomic transition: applications to laser frequency locking. *Journal of Physics B: Atomic, Molecular and Optical Physics*, 35(24):5141, December 2002.

[18] M. L. Harris, C. S. Adams, S. L. Cornish, I. C. McLeod, E. Tarleton, and I. G. Hughes. Polarization spectroscopy in rubidium and cesium. *Physical Review A*, 73(6):062509, June 2006.

[19] V. B. Tiwari, S. Singh, S. R. Mishra, H. S. Rawat, and S. C. Mehendale. Laser frequency stabilization using doppler-free bi-polarization spectroscopy. *Optics Communications*, 263(2):249–255, July 2006.

[20] Huy Diep Do, Geol Moon, and Heung-Ryoul Noh. Polarization spectroscopy of rubidium atoms: Theory and experiment. *Physical Review A*, 77(3):032513, March 2008.

[21] Tzu-Ping Ku, Chi-Yuan Huang, Bor-Wen Shiau, and Dian-Jiun Han. Phase shifting interferometry of cold atoms. *Optics Express*, 19(4):3730, February 2011.

[22] L. D. Turner, K. F. E. M. Domen, and R. E. Scholten. Diffraction-contrast imaging of cold atoms. *Physical Review A*, 72(3):031403, 2005. Copyright (C) 2009 The American Physical Society; Please report any problems to prola@aps.org.